

# Fractional Montgomery effect: a self-imaging phenomenon

Adolf W. Lohmann

Universität Erlangen-Nürnberg, Cauerstrasse 7, 91058 Erlangen, Germany

Hans Knuppertz and Jürgen Jahns

FernUniversität Hagen, Optische Nachrichtentechnik, Universitätsstrasse 27/PRG, 58084 Hagen, Germany

Received December 22, 2004; accepted January 8, 2005

Self-imaging means image formation without the help of a lens or any other device between object and image. There are three versions of self-imaging: the classical Talbot effect (1836), the fractional Talbot effect, and the Montgomery effect (1967). Talbot required the object to be periodic; Montgomery realized that quasiperiodic suffices. Classical means that the distance from object to image is an integer multiple of the Talbot distance  $z_T = 2p^2/\lambda$ , where  $p$  is the grating period. Fractional implies a distance that is a simple fraction of  $z_T$ : say,  $z_T/2, z_T/4, 3z_T/2 \dots$ . We explore the most general case of the fractional Montgomery effect. © 2005 Optical Society of America

OCIS codes: 070.6760, 110.6760, 050.0050.

## 1. HISTORICAL BACKGROUND

Self-imaging means image formation without a lens or any other instrument in the space between the object and the image. The object is illuminated by a monochromatic plane wave. Talbot<sup>1</sup> described such an effect in 1836. His object was a grating in transmission. Lord Rayleigh<sup>2</sup> rediscovered the effect and provided a theoretical explanation. The distance between object and image had to be a Talbot length  $z_T$ , or an integer multiple thereof:

$$z_T = 2p^2/\lambda, \quad p: \text{grating period.} \quad (1)$$

The Talbot distance is typically 4 cm if the light is green and if the grating period is 0.1 mm.

A review article by Paturski<sup>3</sup> and a comprehensive study by Winthrop and Worthington<sup>4</sup> describe the status of research on self-imaging as of 40 years ago. Montgomery<sup>5</sup> found 38 years ago that the classical Talbot effect is only a special case of a larger class of self-imaging effects. The difference between these two effects is that for the Talbot effect the object  $u_T(x)$  has to be periodic:

$$U_T(x) = U_T(x+p) = \sum_m A_m \exp\left(2\pi i m \frac{x}{p}\right). \quad (2)$$

The associated frequency spectrum consists of equidistant peaks:

$$\int U_T(x) \exp(-2\pi i \nu x) dx = \tilde{U}_T(\nu) = \sum_m A_m \delta(\nu - m\nu_0). \quad (3)$$

The basic frequency  $\nu_0$  is the inverse of the grating period  $p$ :

$$\nu_0 = \frac{1}{p}. \quad (4)$$

The Montgomery object is quasiperiodic in the following sense:

$$U_m(x) = B_0 + \sum_{m \neq 0} B_m \exp\left(2\pi i \frac{m}{\sqrt{|m|}} \nu_0 x\right), \quad (5)$$

$$\tilde{U}_M(\nu) = B_0 \delta(\nu) + \sum_{m \neq 0} B_m \delta\left(\nu - \frac{m}{\sqrt{|m|}} \nu_0\right). \quad (6)$$

The term with  $B_1, B_4, B_9 \dots$  does exist as part of the Talbot series [Eq. (3)]. But  $B_2, B_3, B_5 \dots$  are new. Hence the Talbot images constitute only a subset of the Montgomery images.

Cowley and Moodie<sup>6</sup> studied self-imaging in the spirit of Talbot about 50 years ago. They distinguished two cases that they called Fourier images and Fresnel images, respectively. Their Fourier images, observed at distances  $z = Nz_T$  ( $N$  is an integer), are what we call here classical Talbot images, or simply Talbot images. The Fresnel images occur at simple fractions of the Talbot distance:

$$\Delta z = \frac{N}{M} z_T. \quad (7)$$

The  $N$  and  $M$  are small integers, such that the fraction is, e.g.,  $(N/M) = 1/2, 1/4, 2/3$ . We will call these Fresnel images fractional Talbot images. Not every fractional Talbot image resembles the object. It depends on the fraction  $(N/M)$  and the shape of the grating groove. In other words, it depends on the specific set of Fourier coefficients  $A_m$  [Eq. (2)]. The fractional Talbot images will be explained in Section 4.

For now we will briefly explain our preference of the terms Talbot image (instead of Fourier image) and fractional Talbot image (instead of Fresnel image). First, self-imaging was invented by Talbot, not by Fourier. The name Fresnel is not out of place in this context since light propagation in free space is often called Fresnel diffraction. However, the Talbot effect is restricted to periodic objects while Fresnel diffraction does occur at all kinds of aperiodic objects, observed at an arbitrary distance from the object.

So far three effects have been studied thoroughly: the Talbot effect, the fractional Talbot effect, and the Montgomery effect. Having now classified self-imaging in this manner, the obvious target for further studies is the fractional Montgomery effect. Table 1 explains the rationale for expecting the existence of such an effect.

## 2. MOTIVATION AND PLAN

The primary motivation is curiosity, as indicated at the end of Section 1. And we hope that the fractional Montgomery effect might improve some of the existing self-imaging systems that rely so far on the classical Talbot effect. Existing applications of the Talbot effect are noncontact copying,<sup>2</sup> electron microscopy,<sup>6</sup> noise suppression in gratings,<sup>7</sup> image transmission,<sup>8</sup> beam splitting and array illumination,<sup>8–11</sup> interferometry,<sup>12,13</sup> Fourier spectrometry,<sup>14</sup> and temporal information processing.<sup>15</sup> References 6 and 9–11 refer to the fractional self-imaging effect and some of its applications.

Our plan is to formulate the theory of the Talbot effect in a manner that suits our purposes (Section 3). From there we proceed to the fractional Talbot effect (Section 4). Next follows the theory of the Montgomery effect (Section 5). The step from there to the fractional Montgomery effect (Section 6) resembles the fractionalization of the Talbot effect (Section 4). In Section 7 we compare Talbot and Montgomery effects in the framework of the Ewald sphere. In Section 8 we reveal a kinship between the classical Talbot effect and the fractional Montgomery effect. Finally, we summarize and draw some conclusions (Section 9).

## 3. TALBOT EFFECT

The classical Talbot setup is shown in Fig. 1. A grating (as the object) with period  $p$  is illuminated by a monochromatic plane wave. Immediately behind the grating at plane  $z=0$ , the complex amplitude is

$$U(x,0) = \bar{U} + \sum_{m \neq 0} A_m \exp(2\pi i m \nu_0 x) = A_0 + u(x,0). \quad (8)$$

**Table 1. Classification of Self-Imaging Effects**

Periodicity	Distance $z/z_T$	
	Integer	Fractional
Lateral in $x$	Talbot (1836)	Winthrop (1965)
Longitudinal in $z$	Montgomery (1967)	2004

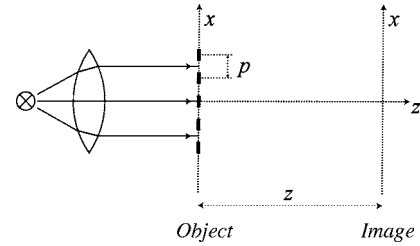


Fig. 1. Talbot setup. A grating with the period  $p$  is the object; the observed image is at distance  $z$ .

It turns out that it is practical to split the mean value  $\bar{U}=A_0$  from the rest of the Fourier series. The spatial-frequency spectrum is

$$\tilde{U}(\nu,0) = A_0 \delta(\nu) + \sum_{m \neq 0} A_m \delta(\nu - m \nu_0) = A_0 \delta(\nu) + \tilde{u}(\nu, z=0). \quad (9)$$

Propagating in free space over the distance  $z$  means to multiply the frequency spectrum by a quadratic phase factor (in paraxial approximation):

$$\exp(-i\pi\lambda z \nu^2) = \exp(-i\pi\lambda z m^2 \nu_0^2), \quad (10)$$

which yields

$$\begin{aligned} \tilde{U}(\nu,z) &= A_0 \delta(\nu) + \sum_{m \neq 0} A_m \exp(-i\pi\lambda z m^2 \nu_0^2) \delta(\nu - m \nu_0) \\ &= A_0 \delta(\nu) + \tilde{u}(\nu,z). \end{aligned} \quad (11)$$

We modify the exponent

$$-i\pi\lambda z m^2 \nu_0^2 = -2\pi i m^2 \frac{z}{z_T}, \quad z_T = \frac{2}{\lambda \nu_0^2} = \frac{2p^2}{\lambda}. \quad (12)$$

Hence

$$\tilde{U}(\nu,z) = A_0 \delta(\nu) + \sum_{m \neq 0} A_m \exp\left(-2\pi i m^2 \frac{z}{z_T}\right) \delta(\nu - m \nu_0). \quad (13)$$

The exponential term in Eq. (13) is periodic in the  $z$  direction as well:

$$\begin{aligned} U(x,z) &= A_0 + \sum_{m \neq 0} A_m \exp\left[2\pi i \left(m \nu_0 x - m^2 \frac{z}{z_T}\right)\right] \\ &= U(x,z + Nz_T). \end{aligned} \quad (14)$$

This is the central equation of the Talbot theory.

## 4. FRACTIONAL TALBOT EFFECT

So far we requested only  $x$  periodicity of the object  $U(x,0)$ . The groove shape and hence the Fourier coefficients were not specified. Now we assume a specific object, a Ronchi grating (Fig. 2):

$$U(x,0) = 1 + \sum_{m \neq 0} \text{sinc}\left(\frac{m}{2}\right) \exp(2\pi i m \nu_0 x) = 1 + \Delta U(x,0). \quad (15)$$

The Fourier coefficients are apparently

$$A_0 = 1; \quad A_m = \text{sinc}\left(\frac{m}{2}\right); \quad A_{2m} = 0. \quad (16)$$

The even-order coefficients are zero, except for  $m=0$ . That is an essential feature, as noted a long time ago, e.g., by Rogers.<sup>16</sup> For  $z > 0$  the complex amplitude is

$$U(x, z) = 1 + \sum_{m \neq 0} \text{sinc}\left(\frac{m}{2}\right) \exp\left[2\pi i\left(m\nu_0 x - m^2 \frac{z}{z_T}\right)\right] = 1 + \Delta U(x, z). \quad (17)$$

Now we enter the domain of the fractional Talbot effect. We compute the complex amplitude at a  $(z_T/2)$  distance from the object plane  $z=0$ :

$$U\left(x, \frac{z_T}{2}\right) = 1 - \sum_{m \neq 0} \text{sinc}\left(\frac{m}{2}\right) \exp(2\pi i m \nu_0 x) = 1 - \Delta U(x, 0). \quad (18)$$

The minus sign arises for  $z=z_T/2$  and  $m$  odd because the  $z$ -dependent phase factor is now

$$\exp\left(-2\pi i \frac{m^2}{2}\right) = -1 \quad (m \text{ odd}). \quad (19)$$

Expressed in the  $x$  domain,

$$U(x, 0) = 1 + \Delta U(x, 0) = 1 + \begin{cases} +1 & \left|x - mp - \frac{p}{4}\right| \leq \frac{p}{2} \\ -1 & \text{otherwise} \end{cases} = \begin{cases} 2 \\ 0 \end{cases}, \quad (20a)$$

$$U\left(x, \frac{z_T}{2}\right) = 1 - \Delta U(x, 0) = 1 - \begin{cases} +1 \\ -1 \end{cases} = \begin{cases} 0 \\ 2 \end{cases}. \quad (20b)$$

The Ronchi grating and its  $(z_T/2)$  fractional Talbot image are shown in Figs. 2 and 3. A comparison of Eq. (15) (Fig. 2) and Eq. (18) (Fig. 3) indicates a contrast reversal. The same contrast reversal can be achieved by a lateral shift ( $p/2$ ):

$$U\left(x, \frac{z_T}{2}\right) = U\left(x + \frac{p}{2}, 0\right). \quad (21)$$

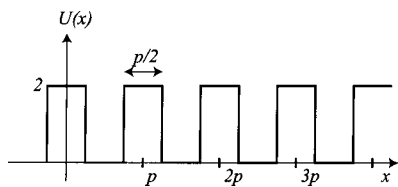


Fig. 2. Ronchi grating.

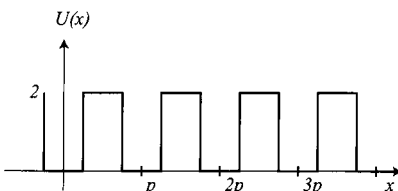


Fig. 3. Fractional Talbot image of a Ronchi grating at a distance  $z=z_T/2$ .

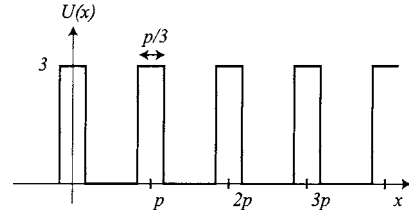


Fig. 4. Close relative of the Ronchi grating with the duty factor (1/3).

The significant feature that caused a contrast reversal was based on  $A_{2m}=0$  (except for  $m=0$ ). The Ronchi grating is only one case of a large variety of objects  $U(x, 0)$  whose even-order Fourier coefficients are zero. It is enough if  $U(x, 0) - U(0, 0)$  is composed of a pair of shifted signals  $v(x)$ :

$$v(x) = \sum_m B_m \exp(2\pi i m \nu_0 x), \quad (22a)$$

$$\begin{aligned} \Delta U(x, 0) &= v\left(x + \frac{p}{4}\right) - v\left(x - \frac{p}{4}\right) \\ &= 2i \sum_m B_m \sin\left(m \frac{\pi}{2}\right) \exp(2\pi i m \nu_0 x). \end{aligned} \quad (22b)$$

The bias term  $B_0$  of  $U(x, 0)$  is not affected by Eqs. (22). We generalize and state that a  $z$  shift by  $M/N$  changes

$$A_m \rightarrow A_m \exp\left[-2\pi i m^2 \left(\frac{M}{N}\right)\right], \quad (23a)$$

and a lateral shift by  $(M'/N') p$  changes

$$A_m \rightarrow A_m \exp\left[-2\pi i m \left(\frac{M'}{N'}\right)\right]. \quad (23b)$$

The effect of  $z=z_T/4$  is the crucial feature of the array illuminator project.<sup>10,11</sup> There the object was a phase Ronchi grating, with a phase step  $\pi/2$ . At a distance  $z=z_T/4$ , the fractional Talbot image is a pure amplitude Ronchi pattern. Another interesting case arises if  $M'/N' = 2(M/N)$ . Now the exponent will be  $-2\pi i (M/N)[(m-1)^2 - 1]$ . The square bracket will be odd if  $m$  is odd and even if  $m$  is even.

A modified Ronchi grating with a duty factor (1/3) has Fourier coefficients such as  $A_{3m}=0$  (Fig. 4). It is tempting now to observe at the fractional plane  $z=z_T/3$  and at a lateral shift of  $\bar{x}=(2/3)p$ .

Yet another tool for the manipulation of Fourier coefficients is a tilt of the illuminating wave:

$$U(x, 0) \rightarrow U(x, 0) \exp(2\pi i \nu_0 x), \quad (24a)$$

$$A_m \rightarrow A_{m-1}. \quad (24b)$$

Formerly, for a Ronchi grating it was  $A_0=1$  and  $A_{2m}=0$ . Now the odd orders will vanish, except for  $m=-1$ .

## 5. MONTGOMERY EFFECT

Montgomery<sup>5</sup> noticed an interesting aspect of the Talbot effect. Talbot and his followers stated that if  $U_0(x)$  is laterally periodic (in  $x$ ), then  $U(x, z)$  is longitudinally periodic (in  $z$ ). The feature of longitudinal periodicity is what self-imaging is all about. Talbot did realize that lateral periodicity is sufficient for self-imaging. Montgomery posed the question “Is lateral periodicity also necessary?” His answer was “Not necessarily.” The more general kind of objects that we call quasiperiodic [Eqs. (5) and (6)] do exhibit longitudinal periodicity as well. When also introducing the  $z$  dependence into Eqs. (5) and (6), one obtains

$$U_M(x, z) = B_0 + \sum_{m \neq 0} B_m \exp \left[ 2\pi i \left( \frac{m}{\sqrt{|m|}} \nu_0 x - |m| \frac{z}{z_T} \right) \right], \quad (25a)$$

$$\begin{aligned} \tilde{U}_M(\nu, z) &= B_0 \delta(\nu) + \sum_{m \neq 0} B_m \exp \left( -2\pi i |m| \frac{z}{z_T} \right) \\ &\times \delta \left( \nu - \frac{m}{\sqrt{|m|}} \nu_0 \right). \end{aligned} \quad (25b)$$

Obviously it is

$$U(x, z_T) = U(x, 0). \quad (26)$$

To justify the step from Eq. (5) to Eqs. (25) one has to subject the  $U_M(x, y)$  to the paraxial wave equation:

$$\frac{\partial^2 U_M(x, z)}{\partial x^2} + 2ik \frac{\partial U_M(x, z)}{\partial z} = 0. \quad (27)$$

The wave equation is satisfied if  $k = 2\pi/\lambda$  and  $z_T = 2p^2/\lambda$ , where  $p = 1/\nu_0$ .

## 6. FRACTIONAL MONTGOMERY EFFECT

In Section 4 we studied the step from the classical Talbot effect to the fractional Talbot effect. The relative distance  $z/z_T$  was generalized from integer to fractional, like  $z/z_T = 1/2$ . That is legal, of course. But the fractional Talbot complex amplitude  $U(x, z = z_T/2)$  may have no similarity with the object  $U(x, z = 0)$ . Hence it may not be justified to call  $U(x, z_T/2)$  an image.

But there exist some specific objects whose fractional Talbot images do indeed resemble the object. For example, the Ronchi grating does appear at  $z = z_T/2$ , but laterally shifted by  $p/2$ , half a period. For the proof, it is essential that the even-order Fourier coefficients are zero:  $A_{2m} = 0$  (except for  $A_0 = \bar{U}$ ). That feature is useful, too, in the context of the fractional Montgomery effect. We insert  $z = z_T/2$  into Eq. (25a). For  $m$  odd it is  $\exp(-2\pi i |m|/2) = -1$ , which yields

$$U_M \left( x, \frac{z_T}{2} \right) = B_0 - \sum_{m \neq 0} B_m \exp \left( 2\pi i \frac{m}{\sqrt{|m|}} \nu_0 x \right). \quad (28)$$

In other words,

$$U_M \left( x, \frac{z_T}{2} \right) = B_0 - \Delta U_M(x, 0), \quad (29)$$

and with Ronchi coefficients  $B_m = \text{sinc}(m/2)$ ,

$$U_M \left( x, \frac{z_T}{2} \right) = 1 - \sum_{m \neq 0} \text{sinc} \left( \frac{m}{2} \right) \cos(2\pi \sqrt{|m|} \nu_0 x). \quad (30)$$

Equation (30) looks almost like the equation that described the fractional Talbot effect, especially for a Ronchi object (Fig. 3) and for a distance  $z = z_T/2$ . However, corresponding Talbot and Montgomery functions look quite different, even if the set of coefficients  $A_m$  (for Talbot) and  $B_m$  (for Montgomery) are alike. A simple example:

$$A_m = B_m = \text{sinc} \left( \frac{m}{2} \right). \quad (31)$$

We place these two functions side by side, i.e. [Figs. 5(a) and 5(b)]:

$$U_T(x, 0) = 1 + \sum_{m \neq 0} \text{sinc} \left( \frac{m}{2} \right) \exp(2\pi i m \nu_0 x), \quad (32a)$$

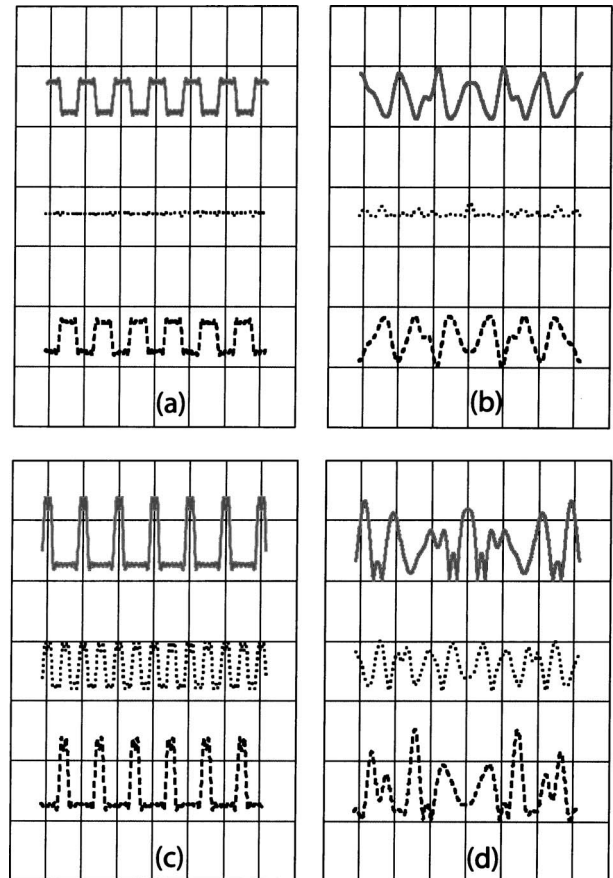


Fig. 5. Lateral field in  $x$  direction generated for (a) Talbot and (b) Montgomery objects at the distances  $z/z_T = 0, 0.25, 0.5$  (top to bottom); in both cases only odd coefficients are relevant. The coefficients used are sinclike with a duty cycle of  $1/2$ ; seven harmonics are used. The lateral field in the  $x$  direction is generated for (c) Talbot and (d) Montgomery objects in the distances  $z/z_T = 0, 0.25, 0.5$  (top to bottom); in both cases odd and even coefficients are relevant. Used coefficients are sinclike with a duty cycle of  $1/4$ ; seven harmonics are used.

$$U_M(x,0) = 1 + \sum_{m \neq 0} \operatorname{sinc}\left(\frac{m}{2}\right) \exp\left(2\pi i \frac{m}{\sqrt{|m|}} \nu_0 x\right). \quad (32b)$$

It is not really interesting to plot the two signals as they occur at half of a Talbot distance, because the structures remain the same. Only the contrasts are reversed:

$$U_T\left(x, \frac{z_T}{2}\right) = 1 - \sum_{m \neq 0} \operatorname{sinc}\left(\frac{m}{2}\right) \exp(2\pi i m \nu_0 x), \quad (33a)$$

$$U_M\left(x, \frac{z_T}{2}\right) = 1 - \sum_{m \neq 0} \operatorname{sinc}\left(\frac{m}{2}\right) \exp\left(2\pi i \frac{m}{\sqrt{|m|}} \nu_0 x\right). \quad (33b)$$

We also show a pair of corresponding signals for a longitudinal shift of  $z_T/4$  but still with the same coefficients [Eqs. (32)].

These curves and a few others in our collection generate the impression of almost chaotic behavior of the Montgomery signals. One may suspect that the change of the integer indices  $m$  into root indices  $m/\sqrt{|m|}$  is the cause. But this process is reversible, as we will see in Section 8. In other words, it is possible to convert those quasi-stochastic Montgomery signals back into well-behaved Talbot signals.

The contrast reversal at  $z = z_T/2$  as described in Eqs. (33a) and (33b) does occur not only if the terms of the series are  $\operatorname{sinc}(m/2)$ . The essence for this contrast reversal is

$$B_{2m} = 0, \quad \text{except } B_0 = \bar{U}_M. \quad (34)$$

That is equivalent to

$$\Delta U_M\left(x, \frac{z_T}{2}\right) = -\Delta U_M(-x, 0). \quad (35)$$

It is apparently sensible to split the sum into a symmetrical ( $S$ ) and antisymmetrical ( $A$ ) part:

$$\sum B_{2m} + \sum B_{2m+1} = U_{M,S}(x,z) + U_{M,A}(x,z). \quad (36)$$

At a fractional location,

$$\Delta U_{M,S}\left(x, \frac{z_T}{2}\right) = +\Delta U_{M,S}\left(-x, \frac{z_T}{2}\right), \quad (37a)$$

$$\Delta U_{M,A}\left(x, \frac{z_T}{2}\right) = -\Delta U_{M,A}\left(-x, \frac{z_T}{2}\right). \quad (37b)$$

A similar sorting of the series is sensible if the location of a plane of observation is  $z = z_T/3$ :

$$\Delta U_M = \sum B_{3m} + \sum B_{3m+1} + \sum B_{3m-1} \dots, \quad (38a)$$

$$\exp[-(2\pi i/3)3m] = 1, \quad (38b)$$

$$\exp[-(2\pi i/3)(3m+1)] = \exp(-2\pi i/3), \quad (38c)$$

$$\exp[-(2\pi i/3)(3m-1)] = \exp(+2\pi i/3). \quad (38d)$$

We now present a strategy for converting an interesting Montgomery object, which may mean a contrast reversal at a location  $z = z_T/2$ :

$$\Delta U_M(x,0) = \bar{U}_M + \Delta U_M(x,0), \quad (39a)$$

$$\Delta U_M\left(x, \frac{z_T}{2}\right) = \bar{U}_M - \Delta U_M(x,0). \quad (39b)$$

We know that the coefficients  $B_{2m}$  ought to be zero for achieving this contrast reversal. We can enforce it by means of spatial filtering, which means that the spectrum  $\tilde{U}_M(\nu, z)$  [see Eq. (25b)] is to be multiplied by

$$\tilde{F}(\nu) = \sin\left[\pi\left(\frac{\nu}{\nu_0}\right)^2\right] = \frac{\exp[+i\pi(\nu/\nu_0)^2] - \exp[-i\pi\left(\frac{\nu}{\nu_0}\right)^2]}{2i}. \quad (40)$$

This filter is zero whenever  $\pi(\nu/\nu_0)^2 = \pi N$ ;  $\nu = \nu_0 \sqrt{N}$ .

We want this to occur at  $\nu = \nu_1 \sqrt{2m}$  because we want to eliminate the even-order coefficients  $B_{2m}$ . Hence  $\nu_0 = \nu_1 \sqrt{2}$  is the proper zero location in the frequency domain.

A filter with a quadratic phase such as  $-\pi\lambda z \nu^2$  is known to shift the wave front by an amount  $z$  in the axial direction. The two exponentials will virtually shift the signal to the opposite directions by  $\pm 1/(\lambda \nu_0^2) = \pm z_T/2$ . A similar filter generates three versions of the signal at  $z=0$  and at  $\pm 2/(\lambda \nu_0^2)$ :

$$\tilde{F}(\nu) = 1 - \cos\left[\frac{\pi}{2}\left(\frac{\nu}{\nu_0}\right)^2\right]. \quad (41)$$

## 7. UNIFIED EXPLANATION OF THE EFFECTS DUE TO TALBOT AND MONTGOMERY EFFECTS

Talbot self-imaging is a special case of the more general Montgomery effect; therefore it is of interest to find a unified explanation for both. A formulation that was based on the McCutchen theorem<sup>17</sup> was presented by Indebetouw.<sup>18</sup> The kinship between Montgomery and McCutchen will also be commented on in Section 8. Here we want to use the concept of the Ewald sphere to clarify the relationship between the two effects, those due to Talbot and those due to Montgomery.

It turns out to be profitable if we translate the problem from the 3D space domain  $(x, y, z)$  into the 3D spatial-frequency domain. We start with the rigorous Helmholtz equation for monochromatic light:

$$\Delta V(x, y, z) + k^2 V(x, y, z) = 0, \quad k = 2\pi/\lambda. \quad (42)$$

Every 3D function can be decomposed into Fourier elements:

$$V(x, y, z) = \int \int \int \tilde{V}(\nu_x, \nu_y, \nu_z) \times \exp[2\pi i(x\nu_x + y\nu_y + z\nu_z)] d\nu_x d\nu_y d\nu_z. \quad (43)$$

We insert this Fourier decomposition into the Helmholtz

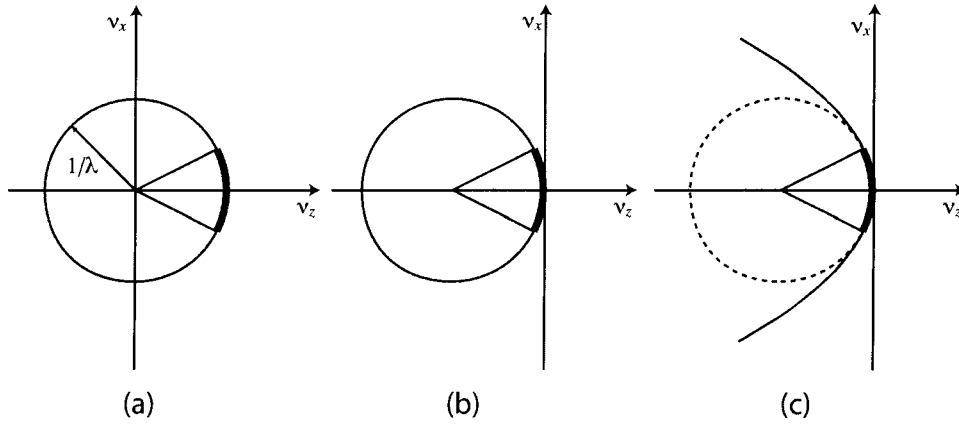


Fig. 6. (a) Ewald sphere, (b) shifted Ewald sphere, (c) paraboloid, paraxial approximation.

equation, which now appears as

$$\int \int \int [-(2\pi)^2(\nu_x^2 + \nu_y^2 + \nu_z^2) + k^2] \tilde{V}(\nu) \times \exp(2\pi i \nu x) d\nu_x d\nu_y d\nu_z = 0. \quad (44)$$

The argument of the exponential is an abbreviation of the exponent in Eq. (43). The value zero in Eq. (44) for everywhere in  $(x, y, z)$  is assumed if the square bracket or the Fourier transform  $\tilde{V}(\nu)$  vanishes. In other words, the 3D spatial-frequency spectrum  $\tilde{V}(\nu)$  is allowed to be non-zero only on a sphere, which is named after Ewald [Fig. 6(a)].

$$\nu_x^2 + \nu_y^2 + \nu_z^2 = (1/\lambda)^2. \quad (45)$$

In other words, every point of this sphere represents a legal wave vector of length  $2\pi/\lambda$ . We assume the  $z$  axis as the optical axis of our experimental setup. Existing wave vectors will deviate usually from the  $\nu_z$  axis only by a finite angle, in Fig. 6(a), for example, by  $\pm 45^\circ$ . We can consider the particular wave vector that is parallel to the  $\nu_z$  axis as a carrier frequency. Hence we extract it from the complex amplitude  $V$ :

$$V(x, y, z) = u(x, y, z) \exp\left(2\pi i \frac{z}{\lambda}\right). \quad (46)$$

The Ewald sphere  $\tilde{u}(\nu_x, \nu_y, \nu_z)$  belonging to  $u(x, y, z)$  is now shifted such that the origin  $(\nu_x=0, \nu_y=0, \nu_z=0)$  is touched [Fig. 6(b)]. The shift of the Ewald sphere to the left implies that the carrier wave  $\exp(ikz)$  propagates in the plus  $z$  direction:

$$\nu_x^2 + \nu_y^2 + (\nu_z + 1/\lambda)^2 = (1/\lambda)^2. \quad (47)$$

Equation (47) is illustrated in Fig. 6(b). The modified Helmholtz equation for  $u(x, y, z)$  is

$$\Delta_{xy} u(x, y, z) + 2ik \frac{\partial u(x, y, z)}{\partial z} = 0. \quad (48)$$

This wave equation is still exact. The paraxial approximation therefore allows us to disregard the second-order  $z$  derivative:

$$\frac{\partial^2 u(x, y, z)}{\partial z^2} \approx 0. \quad (49)$$

Hence the wave equation is now

$$\Delta_{xy} u(x, y, z) + 2ik \frac{\partial u(x, y, z)}{\partial z} = 0. \quad (50)$$

A translation of the approximation in approximation (49) into the spatial-frequency domain means to drop the term  $\nu_z^2$  in Eq. (47). Hence the off-center Ewald sphere [Fig. 6(b)] becomes a paraboloid [Fig. 6(c)]:

$$\nu_x^2 + \nu_y^2 + 2\frac{\nu_z}{\lambda} = 0. \quad (51)$$

We drop one of the lateral variables, the  $y$ , for the sake of simplicity without losing much generality. As a consequence we also drop the  $\nu_y$  in Eq. (51), which reads

$$\nu_x^2 + 2\frac{\nu_z}{\lambda} = 0. \quad (52)$$

That parabola indicates which spatial frequencies  $(\nu_x, \nu_y)$  are allowed by the wave equation.

We now restrict the range of feasible spatial frequencies even further by invoking lateral periodicity of the wave field:

$$U(x, y) = \sum_n U_n(z) \exp(2\pi i n \nu_0 x). \quad (53)$$

The associated Fourier representation is

$$\tilde{U}(\nu_x, \nu_y) = \sum_n \tilde{U}_n(\nu_z) \delta(\nu_x - n\nu_0). \quad (54)$$

These are parallel equidistant sheets in the spatial-frequency domain, as shown in Fig. 7. The crossover points indicate those spatial frequencies that are legalized by the wave equation [Eq. (52)] and that indicate lateral periodicity [Eq. (53)]. The combination of Eqs. (52) and (53) describes the scenery of the Talbot effect, illustrated in the Fourier domain by the solid circles.

We want to know the longitudinal period  $\rho$  of the wave field. We insert the periodicity condition  $\nu_x = n\nu_0$  into the wave condition [Eq. (52)] and obtain

$$v_z = -n^2 \lambda \frac{v_0^2}{2} = -n^2 \rho, \tag{55}$$

$$\frac{1}{\rho} = z_T = \frac{2}{\lambda v_0^2} = 2 \frac{\rho^2}{\lambda}. \tag{56}$$

So far lateral periodicity was the cause and longitudinal periodicity was the consequence. That is Talbot's point of view. Now, in the spirit of Montgomery, we demand longitudinal periodicity:

$$v_z = -m\rho. \tag{57}$$

The circles in Fig. 8 indicate how this demand may be compatible with the wave equation [Eq. (52)]. We find

$$v_x^2 = -2m \frac{\rho}{\lambda}. \tag{58}$$

The lateral locations of the circles are

$$v_m = \sqrt{m} v_1 = \sqrt{m} \rho \tag{59}$$

shown in Fig. 8.

Figures 7 and 8 are combined in Fig. 9. Open circles belong to both the Talbot and the Montgomery set. The solid circles belong only to the Montgomery set. This proves

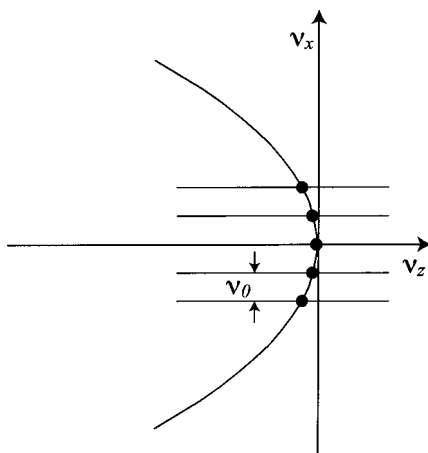


Fig. 7. Talbot effect in the spatial-frequency domain.

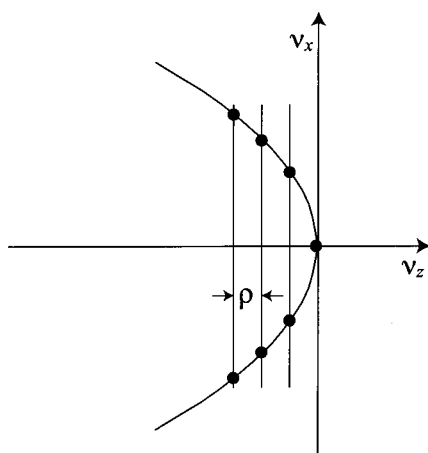


Fig. 8. Montgomery effect in the spatial-frequency domain.

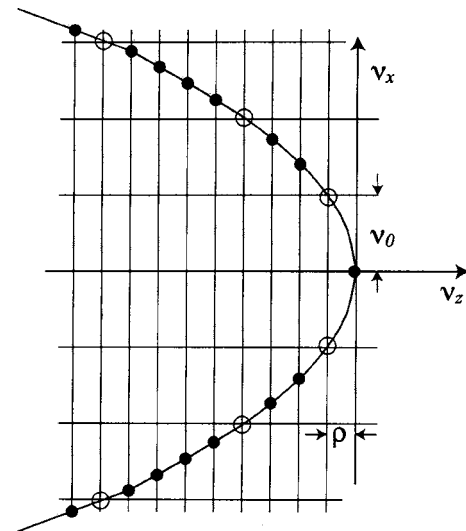


Fig. 9. Peaks of the Talbot effect (open circles) and of the Montgomery effect (solid circles);  $v_0$  is the lateral periodicity;  $\rho$  is the longitudinal periodicity.

that the Montgomery effect is much richer. The Talbot effect represents only a subset.

### 8. KINSHIP BETWEEN THE CLASSICAL TALBOT EFFECT AND THE FRACTIONAL MONTGOMERY EFFECT

We compare the wave fields of the classical Talbot effect [Eq. (14)] and of the fractional Montgomery effect [Eqs. (25)]:

$$U_T(x,z) = A_0 + \sum_{m \neq 0} A_m \exp \left[ 2\pi i \left( m v_0 x - m^2 \frac{z}{z_T} \right) \right], \tag{60}$$

$$U_M(x,z) = B_0 + \sum_{m \neq 0} B_m \exp \left[ 2\pi i \left( \frac{m}{\sqrt{|m|}} v_0 x - |m| \frac{z}{z_T} \right) \right]. \tag{61}$$

We notice that the running index  $m$  appears as

$$(m, m^2) \text{ for Talbot and } \left( \frac{m}{\sqrt{|m|}}, |m| \right) \text{ for Montgomery.} \tag{62}$$

The two wave fields will depend only on the linear version  $m$  of the index if  $z/z_T$  is an integer and if it is  $x=0$  in the Montgomery case.

$$U_T(x, z = Nz_T) = U_T(x, z = 0) = A_0 + \sum_{m \neq 0} A_m \exp[2\pi i(m v_0 x)], \tag{63a}$$

$$U_M(x = 0, z) = B_0 + \sum_{m \neq 0} B_m \exp \left( -2\pi i |m| \frac{z}{z_T} \right). \tag{63b}$$

Apparently, the lateral structure of the Talbot object [Eq. (63a)] is the same as the longitudinal structure of the

fractional Montgomery field on the optical  $z$  axis [Eq. (63b)]. These two expressions are identical if the coefficients are the same:

$$A_m = B_{-m}. \quad (64)$$

The periods are  $p=1/\nu_0$  in the Talbot case and  $z_T = 2p^2/\lambda$  in the Montgomery case. The two periods scale as

$$z_T/p = 2p/\lambda. \quad (65)$$

The kinship as expressed by Eqs. (60) and (61) may be helpful if a particular  $z$  dependence of the Montgomery field is wanted.

The question may arise as to whether this kinship could have been also derived in another way by invoking the McCutchen theorem.<sup>17,18</sup> The answer is yes, in a certain way that is presented now. The setup (Fig. 10) considered by McCutchen contains a rotational symmetric pupil  $P$ . The transmission of this pupil, when expressed as a function of radius square, is the Fourier transformation of the complex amplitude on the optical  $z$  axis.

Or the other way around, the complex amplitude  $U(x,y,z)$  on the optical axis ( $x=0; y=0$ ) is the Fourier transform of the pupil function  $\tilde{P}$ :

$$U(0,0,z) = \int \tilde{P}(r^2) \exp\left(-i\pi \frac{z}{\lambda f^2} r^2\right) d(r^2). \quad (66)$$

This complex amplitude will be periodic in  $z$ , if the pupil function is structured like

$$\tilde{P}(r^2) = \sum_{m>0} A_m \delta(r^2 - mr_1^2) = \sum_{m>0} A_m \delta(r - \sqrt{m}r_1). \quad (67)$$

In other words, the pupil function is assumed to consist of concentric rings with radii

$$r_m = r_1 \sqrt{m}, \quad m = 0, 1, 2, \dots \quad (68)$$

A subset of these rings with  $m=0, 1, 4, 9, \dots$  will also cause the complex amplitude  $U(0,0,z)$  to be periodic in  $z$ .

The essence of the McCutchen theorem is the Fourier relationship between  $\tilde{P}(r^2)$  and  $U(0,0,z)$ . Periodicity in  $z$  is a special case in the spirit of Montgomery. One difference of the McCutchen approach is that he uses radius and angle as coordinates while we preferred to use Cartesian coordinates. Furthermore, McCutchen is interested only in the optical  $z$  axis itself whereas we are concerned about images in the  $(x,y)$  planes at various depth  $z$  locations. The fractional Talbot effect is probably the closest relative; a lateral quasiperiodicity is the cause of a longitudinal periodicity.

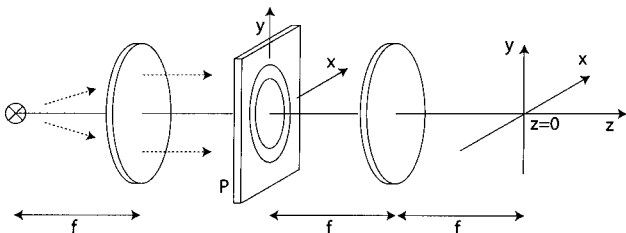


Fig. 10. Setup underlying the McCutchen theorem.

## 9. CONCLUSIONS

The goal of this study was to explore self-imaging in a broad way. The generality is not total since we did not cover aspects of polarization,<sup>19–21</sup> of partial coherence,<sup>3,22,23</sup> and of temporal effects.<sup>15,24</sup> The temporal effects are relevant in the terahertz domain and beyond.

Most projects so far rely on the classical Talbot effect. That implies several restrictions: periodic objects and observation only at a Talbot distance  $z_T$  or an integer multiple thereof. The fractional Talbot effect has more design parameters since the  $z$  distance may now be a fraction of  $z_T$ , say  $z_T/2, z_T/4, \dots$ . Some of the applications mentioned in this paper are impossible without the possibility to use fractional distances.

The step from the classical Talbot effect to the classical Montgomery effect increases the number of design parameters considerably, as became evident when we studied the admissible spots on the Ewald paraboloid. Among the Montgomery coefficients  $B_m$  [Eq. (61)], only  $B_1, B_4, B_9, \dots$  are also among the Talbot coefficients. But  $B_2, B_3, B_5, B_6, B_7, B_8, \dots$  arises only in the context of the Montgomery effect. Expressed in another way, the set of acceptable objects does extend beyond periodic objects to quasi-periodic objects.

The step from the classical Montgomery effect to the fractional Montgomery effect allows us to replace the distance  $z_T$  by  $z_T(N/M)$ . As a consequence, a coefficient  $B_m$  can now be generalized:

$$B_m \rightarrow B_m \exp\left(2\pi i m \frac{N}{M}\right). \quad (69)$$

The gain in design freedom may be comparable to what was achieved when the Talbot effect was fractionalized. To explore the advantages when generalizing the classical Talbot effect may benefit from number theory.

A few generalizations are postponed here: two-dimensional objects,<sup>25</sup> especially those that benefit from polar coordinates;<sup>26,27</sup> the effect of partial coherence;<sup>3,22,23</sup> and temporal aspects of self-imaging.<sup>15,24</sup> Nevertheless, we hope to have shown that self-imaging is more than the classical Talbot effect.

## REFERENCES

1. H. F. Talbot, "Facts relating to optical science, No. IV," *Philos. Mag.* **9**, 401–407 (1836).
2. Lord Rayleigh, "On copying diffraction gratings and on some phenomenon connected therewith," *Philos. Mag.* **11**, 196–205 (1881).
3. K. Patorski, "The self-imaging phenomenon and its applications," *Prog. Opt.* **27**, 1–108 (1989).
4. J. T. Winthrop and C. R. Worthington, "Theory of Fresnel images. I. Plane periodic objects in monochromatic light," *J. Opt. Soc. Am.* **55**, 373–381 (1965).
5. W. D. Montgomery, "Self-imaging objects of infinite aperture," *J. Opt. Soc. Am.* **57**, 772–778 (1967).
6. J. Cowley and A. Moodie, "Fourier images IV: the phase grating," *Proc. Phys. Soc. London* **76**, 378–384 (1960).
7. H. Dammann, G. Groh, and M. Kock, "Restoration of faulty images of periodic objects by means of self-imaging," *Appl. Opt.* **10**, 1454–1455 (1971).
8. O. Bryngdahl, "Image formation using self-imaging techniques," *J. Opt. Soc. Am.* **63**, 416–418 (1973).
9. R. Ulrich and T. Kamiya, "Resolution of self-image in

- planar optical waveguides," J. Opt. Soc. Am. **68**, 583–592 (1978).
10. A. W. Lohmann, "An array illuminator based on the Talbot effect," *Optik (Stuttgart)* **79**, 41–45 (1988).
  11. A. W. Lohmann and J. A. Thomas, "Making an array illuminator based on the Talbot effect," *Appl. Opt.* **29**, 4337–4340 (1990).
  12. A. W. Lohmann and D. E. Silva, "An interferometer based on the Talbot effect," *Opt. Commun.* **2**, 413–415 (1971).
  13. S. Yokozeiki and T. Suzuki, "Shearing interferometer using the grating as the beam splitter," *Appl. Opt.* **10**, 1575–1580 (1971).
  14. A. W. Lohmann, "A new Fourier spectrometer consisting of a two-grating-interferometer (resonance effects between two diffraction gratings in series)," in *Proceedings of the International Commission for Optics Conference on Optical Instruments* (International Commission for Optics, 1962), pp. 58–61.
  15. J. Jahns, E. ElJoudi, D. Hagedorn, and S. Kinne, "Talbot interferometer as a time filter," *Optik (Stuttgart)* **112**, 295–298 (2001).
  16. G. L. Rogers, "Interesting paradox in Fourier images," *J. Opt. Soc. Am.* **62**, 917–918 (1972).
  17. C. W. McCutchen, "Generalized aperture and the three-dimensional diffraction image," *J. Opt. Soc. Am.* **54**, 240–244 (1964).
  18. G. Indebetouw, "Polychromatic self-imaging," *J. Mod. Opt.* **35**, 243–252 (1988).
  19. F. Gori, "Measuring Stokes parameters by means of a polarization grating," *Opt. Lett.* **24**, 584–586 (1999).
  20. J. Tervo and J. Turunen, "Transverse and longitudinal periodicities in fields produced by polarization gratings," *Opt. Commun.* **190**, 51–57 (2001).
  21. Z. Bomzon, G. Biener, V. Kleiner, and E. Hasman, "Spatial Fourier-transform polarimetry using space-variant subwavelength metal-stripe polarizers," *Opt. Lett.* **26**, 1711–1713 (2001).
  22. E. Lau, "Beugungerscheinung an Doppelrastern," *Ann. Phys.* **6**, 417–427 (1948).
  23. J. Jahns and A. W. Lohmann, "The Lau effect (a diffraction experiment with incoherent illumination)," *Opt. Commun.* **28**, 263–267 (1979).
  24. J. Jahns, H. Knuppertz, and A. W. Lohmann, "Montgomery self-imaging effect using computer-generated diffractive optical elements," *Opt. Commun.* **225**, 13–17 (2003).
  25. A. W. Lohmann and D. E. Silva, "A Talbot interferometer with circular gratings," *Opt. Commun.* **4**, 326–328 (1972).
  26. P. Szwaykowski, "Self-imaging in polar coordinates," *J. Opt. Soc. Am. A* **5**, 185–191 (1988).
  27. P. Szwaykowski and K. Patorski, "Moire fringes by evolute gratings," *Appl. Opt.* **28**, 4679–4681 (1989).